Resource

Cell Chemical Biology

Bioactive Compound Screen for Pharmacological Enhancers of Apolipoprotein E in Primary Human Astrocytes

Highlights

- A screen for apoE-promoting compounds was performed using human primary astrocytes
- Multiple compounds regulate apoE secretion via novel mechanisms
- Small-molecule modulators of DHCR7 and DHCR24 increase apoE secretion
- Microdialysis study validates in vivo activities of identified apoE enhancers

Authors

Gina M. Finan, Ronald Realubit, Sungkwon Chung, ..., John R. Cirrito, Charles Karan, Tae-Wan Kim

Correspondence

twk16@cumc.columbia.edu

In Brief

Finan et al. established a phenotypic high-throughput screen identifying compounds that increase apolipoprotein E secretion in primary human astrocytes via previously unknown mechanisms. These newly identified compounds are active preferentially in human astrocytes, furnishing new tools for investigating apoE biology.

Finan et al., 2016, Cell Chemical Biology *23*, 1526–1538
December 22, 2016
http://dx.doi.org/10.1016/j.chembiol.2016.10.015

Please cite this article as: Finan et al., Bioactive Compound Screen for Pharmacological Enhancers of Apolipoprotein E in Primary Human Astrocytes, Cell Chemical Biology (2016), http://dx.doi.org/10.1016/j.chembiol.2016.10.015

Bioactive Compound Screen for Pharmacological Enhancers of Apolipoprotein E in Primary Human Astrocytes

Gina M. Finan,[1] Ronald Realubit,[2] Sungkwon Chung,[3] Dieter Lütjohann,[4] Nan Wang,[5] John R. Cirrito,[6] Charles Karan,[2] and Tae-Wan Kim[1,7,*]

[1]Department of Pathology and Cell Biology, Taub Institute for Research on Alzheimer's Disease and the Aging Brain, Columbia University Medical Center, 630 West 168th Street, P&S12-430, New York, NY 10032, USA
[2]High Throughput Screening Center, Judith P. Sulzberger Genome Center, Columbia University Medical Center, New York, NY 10032, USA
[3]Department of Physiology, Sungkyunkwan University School of Medicine, Samsung Biomedical Research Institute, Suwon 440-746, South Korea
[4]Institute for Clinical Chemistry and Clinical Pharmacology, University of Bonn, 53127 Bonn, Germany
[5]The Division of Molecular Medicine, Department of Medicine, Columbia University Medical Center, New York, NY 10032, USA
[6]Department of Neurology, Washington University School of Medicine, St. Louis, MO 63110, USA
[7]Lead Contact
*Correspondence: twk16@cumc.columbia.edu
http://dx.doi.org/10.1016/j.chembiol.2016.10.015

SUMMARY

Pharmacological screening in physiologically relevant brain cells is crucial for identifying neuroactive compounds that better translate into in vivo biology and efficacious therapeutics. Pharmacological enhancement of apolipoprotein E (apoE), a cholesterol-transporting apolipoprotein, has been proposed as a promising therapeutic approach for Alzheimer's disease. Several nuclear receptor agonists were initially shown to increase brain apoE levels together with ATP-binding cassette transporter 1 (ABCA1), but their underlying mechanisms remain unclear. To gain an insight on brain apoE regulation, we performed an unbiased high-throughput screening of known drugs and bioactive compounds in cultured human primary astrocytes, the major apoE-producing cell type in the brain. We have identified several small molecules that increase apoE secretion via previously unknown mechanisms, including those not co-inducing ABCA1. These newly identified compounds are active preferentially in human astrocytes but not in an astrocytoma cell line, furnishing new tools for investigating biological pathways underlying brain apoE production.

INTRODUCTION

With rising life expectancy and a growing elderly population, no approved disease-modifying therapeutics, and a weak pipeline of drugs under development, safe and effective treatments for Alzheimer's disease (AD) represents one of the biggest unmet needs in medicine. Extensive genetic, neuropathological, and biochemical studies collectively suggest that cellular pathways modulating apolipoprotein E (apoE) are critically involved in the pathophysiology of AD. ApoE is a major apolipoprotein of high-density lipoprotein (HDL) that mediates cholesterol transport in the brain (Pitas et al., 1987). The human apoE gene has three alleles (*APOE* ε*2*, ε*3*, and ε*4*), resulting in three isoforms of apoE: *apoE2*, *apoE3*, and *apoE4*. The ε*4* allele of the gene encoding human apoE underlies the single most prominent risk factor for late-onset AD and is heavily enriched in AD patient populations, whereas the ε*2* allele appears to be protective. *APOE* ε*3* presents in the majority of the human population with roughly 79% allelic frequency and does not appear to affect AD risk (Corder et al., 1993; Kim et al., 2009; Liu et al., 2013; Mahley and Huang, 2012). Although the underlying mechanisms of apoE in AD are still unfolding, many data suggest that apoE4 contributes to AD pathogenesis. Pathogenic mechanisms of apoE4 act through both amyloid β-peptide (Aβ)-dependent and -independent mechanisms, including the regulation of Aβ clearance, direct modulation of Aβ-producing secretases, blood-brain barrier integrity, neurite outgrowth, synaptic structure and plasticity, neuroinflammation, and neuronal susceptibility against injury or stress (Bellosta et al., 1995; Chen et al., 2012; Guo et al., 2004; Holtzman et al., 1995; Hu et al., 1998; Keene et al., 2011; Kim et al., 2014; LaDu et al., 2001; Leduc et al., 2010; Lynch et al., 2001; Mahley and Huang, 2012; Nathan et al., 1994; Stansley et al., 2012; Tai et al., 2015; Zlokovic, 2013).

ApoE is mainly secreted from astrocytes in the brain, forming HDL-like particles. ATP-binding cassette transporters A1 (ABCA1) and G1 (ABCG1) in the brain mediate the transfer of phospholipids and cholesterol for the lipidation of apoE and influence apoE secretion (Pitas et al., 1987; Vance and Hayashi, 2010; Wahrle et al., 2004). Much evidence indicates that lipidated apoE binds Aβ and facilitates receptor-mediated endocytosis and degradation. In addition, apoE exhibits isoform-specific binding to Aβ and affects apoE-mediated Aβ clearance. The binding affinity of apoE isoforms to Aβ was found to correlate inversely to the risk of developing AD, and it is believed that apoE2 and apoE3 (the most common isoform) facilitates Aβ clearance from the brain (Kim et al., 2009; Saunders et al., 1993; Strittmatter et al., 1993; Yu et al., 2014). As such, an

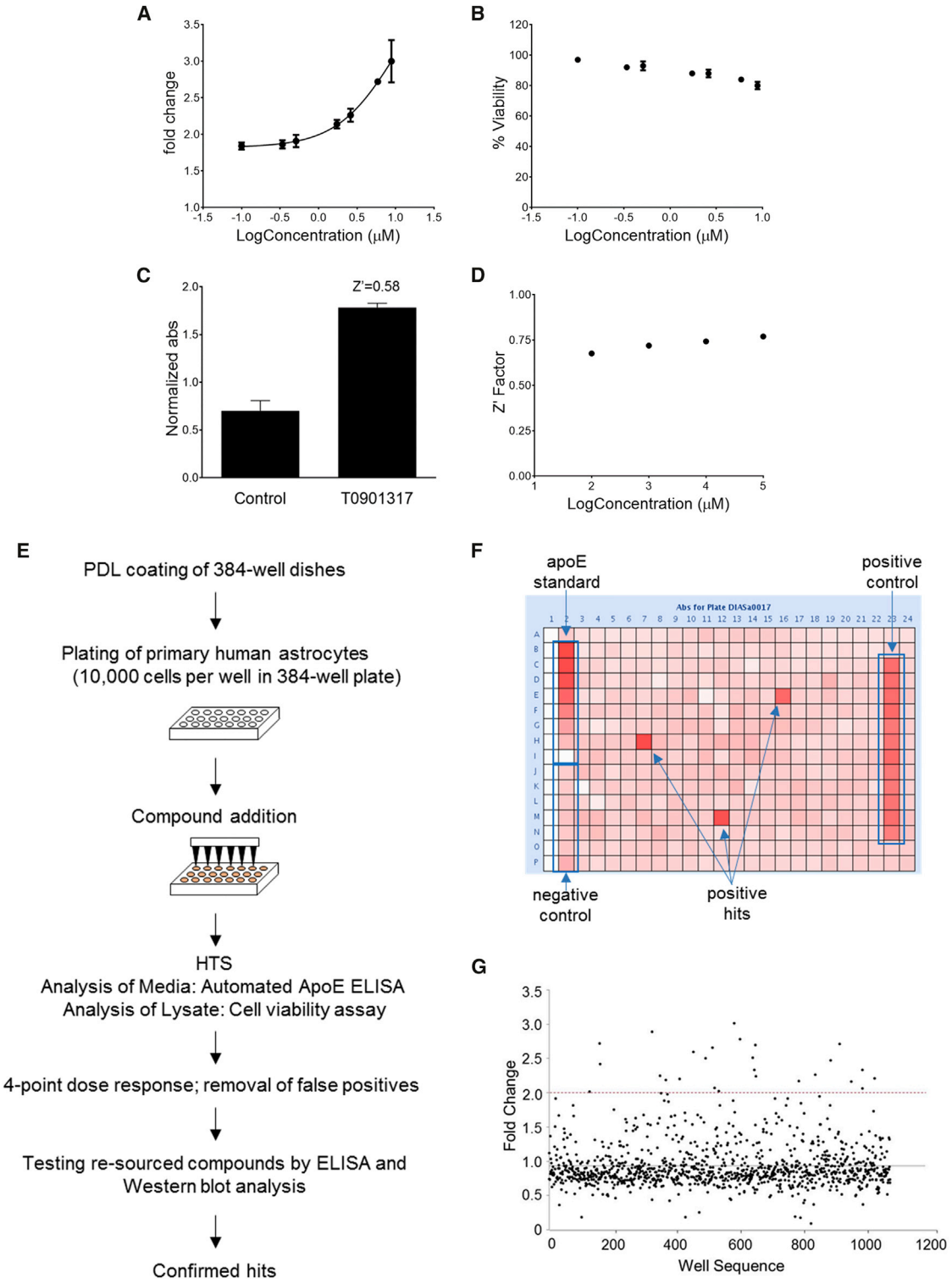

Figure 1. ApoE Assay Optimization and HTS for ApoE-Enhancing Small Molecules in Human Primary Astrocytes

(A) T0901317 dose-response curve. Human astrocytes were treated for 48 hr with increasing doses of T0901317. ApoE was detected using a human apoE ELISA kit (Mabtech). Data points represent mean ± SD, n = 5. ApoE standard range for this ELISA was 0.1–10 ng/mL.

(B) Cell viability of the dose-response curve. Cell viability was determined using CellTiter-Glo. Data points represent mean ± SD, n = 5.

(C) Relative apoE levels (indicated by absorbance) and Z′ calculation for T0901317 at 6 μM, compared with control (mean ± SD), n = 5.

(D) Z′ calculation for T0901317 with an increasing number of wells.

(legend continued on next page)

increase in the levels of functional apoE (the apoE3 isoform) is likely to be beneficial for AD.

ABCA1/G1 is shown to be regulated by nuclear liver X receptors (LXR) or retinoid X receptors (RXR), and promotes secretion and lipidation of apoE (Hong and Tontonoz, 2014; Koldamova et al., 2010; Vance and Hayashi, 2010). Induction of ABCA1 appears to enhance lipidation of apoE and may contribute to the β-amyloid-reducing pharmacological effects of LXR and RXR agonists. LXR agonist T0901317 and RXR agonist bexarotene can cause increased clearance of brain interstitial fluid (ISF) Aβ by promoting apoE production in mouse models of AD (Cramer et al., 2012; Fitz et al., 2014; Fitz et al., 2010, 2013). However, conflicting data have been reported on the effects of bexarotene on plaque brain pathology and cognition in the mouse model (LaClair et al., 2013; Pierrot et al., 2015; Tai et al., 2014). Despite the pathophysiological importance of apoE in AD, the regulatory mechanisms of apoE production and secretion in the brain are still poorly understood. Furthermore, since LXR and RXR agonists induce a number of genes other than apoE, and have widespread physiological effects, it is worthwhile to consider alternative approaches to modulating apoE secretion (Dawson and Xia, 2012; Gabbi et al., 2014).

It is noteworthy that the majority of apoE enhancers were discovered in studies using cell lines, often in macrophages (peripheral immune cells), in the context of atherosclerosis (Kockx et al., 2008; Phillips, 2014). Importantly, no attempts have been made to discover pharmacological agents that regulate apoE secretion in the context of physiological human brain cells, which may facilitate efforts to explore complex underlying biological pathways. To this end, we took an unbiased approach to the discovery of new pharmacological agents that can induce apoE levels in primary human astrocytes. It is highly conceivable that the use of primary human astrocytes for phenotypic screening offers enhanced physiological relevance and greater potential for discovering small-molecule therapeutics with the promise of a favorable translation to humans.

RESULTS

Establishment of an HTS Assay for ApoE Using Primary Human Astrocytes

We chose to use cryopreserved primary human astrocytes, harvested and quality controlled through a commercial vendor, which have been used widely for cell biological investigations (Ruiz et al., 2010). Astrocytes were characterized by immunocytochemistry with antibodies to several well-established astrocytic markers, including glial fibrillary acidic protein (GFAP), GLAST-1, and CD44 (Figure S1A). We also confirmed that the astrocytes were negative for neuronal markers TUJ1 and MAP2 (Figure S1A), as well as microglial marker CD11b and glial progenitor marker NG2 (results not shown). To test the pharmacological responses of these astrocytes, we treated the cells with T0901317, an LXR activator that is known to upregulate established LXR target genes, including apoE and ABCA1 (Liang et al., 2004). Upon T0901317 treatment of these astrocytes, the levels of secreted apoE and cell-associated ABCA1 expression were increased (Figures S1B and S1C).

To establish a high-throughput screening (HTS) assay for the detection of secreted apoE in a 384-well plate format, we determined optimal seeding density (10,000 cells per well) and used a sensitive anti-human apoE antibody for endogenous apoE screening by sandwich ELISA. Parallel detection of apoE (by ELISA) and cell viability was robust upon treating the astrocytes with increasing doses of T0901317 (Figures 1A and 1B). The assay was conducted using replicate wells and exhibited Z′ factors all above 0.58, indicating the robustness of the optimized HTS assay (Figures 1C and 1D).

Primary HTS

A primary screen was performed using a 7,284-compound collection consisting of known drugs, clinical drug candidates, and other bioactive compounds (Table S1). As illustrated in the workflow of the primary screen (Figure 1E), astrocytes were plated in poly-D-lysine-coated 384-well culture dishes and the medium was removed and replaced with medium containing library compounds (10 μM). After a 48-hr incubation with the compounds, the medium was subjected to apoE ELISA, and the remaining cells were analyzed for viability. The genotype of primary screening cells was *APOE3*/3. Each assay plate consists of a human apoE standard along with wells containing negative (DMSO) and positive (T0901317) controls, and the edge wells were not used to maintain assay consistency (Figure 1F). A scatterplot of the fold changes of secreted apoE compared with control (DMSO) from representative screening results of the LOPAC library (1,280 compounds) shows that the mean fold change is 0.93 (Figure 1G). The red dotted line defines the "hit" threshold, which is defined as a fold change greater than 2.0 (~3 SD). From the initial screen, primary hits were confirmed using a 4-point dose-response HTS assay. From the primary screen and validation assay, we identified 69 positive hits. Accordingly, the hit rate was 0.95% (Table S2). We then determined a 7-point dose-response curve of selected confirmed hits using compounds sourced from a second vendor. The corresponding median effective concentration (EC_{50}) values were calculated (Table 1).

Small-Molecule Modulators of DCHR24 and DHCR7 Promote ApoE Secretion in an ABCA1-Independent Manner

Analysis of the confirmed hits with known biological mechanisms or cellular targets revealed several notable pathways similar or identical to putative biological mechanisms functionally linked to apoE secretion (Table 1). For example, several of our identified apoE-promoting compounds are known regulators of cholesterol biosynthesis. U18666A and triparanol are well-known inhibitors of 3β-hydroxysterol Δ(24)-reductase (DHCR24), which catalyzes the conversion of desmosterol to cholesterol (Table 1 and Figure S3) (Zerenturk et al., 2013). GF109203X is a protein

(E) Workflow of small-molecule HTS for apoE enhancers in primary human astrocytes.
(F) A representative assay plate consisting of samples, apoE standard, and positive and negative (DMSO) controls.
(G) Scatterplot of the LOPAC library screen (1,280 compounds) assayed via apoE ELISA at 10 μM in 384-well plates, using primary human astrocytes. "Hits" are defined as a fold change greater than 2.0 (~3 SD), red dotted line. Mean fold change of library = 0.93, black line.

Table 1. Major Target Classes Discovered via HTS in Primary Human Astrocytes

Target Class	Compound	Description	EC_{50} (μM)	Maximal Effect (Fold Change)	ABCA1 Induction
Cholesterol biosynthesis	U18666A	DHCR24 inhibitor	2.35	3.68	no
	triparanol	DHCR24 inhibitor	5.46	5.10	no
	GF109203X	DHCR24 inhibitor	3.42	5.37	no
	AY9944	DHCR7 inhibitor	4.12	4.77	no
	GANT61	DHCR7 agonist	7.33	5.37	no
	haloperidol	DHCR7 inhibitor	8.63	5.53	no
	chlorpromazine	DHCR7 inhibitor	12.25	2.70	no
	clozapine	DHCR7 inhibitor	14.34	2.20	no
	N-desmethylclozapine	DHCR7 inhibitor	11.09	2.00	no
G-protein-coupled receptors	SB65710	urotensin II receptor antagonist	8.57	2.64	yes
	SB611812	urotensin II receptor antagonist	NA	NA	yes
	GSK 1562590	urotensin II receptor antagonist	4.04	2.65	yes
	carvediol	blocker of β1-, β2-, α1-adrenergic receptors	7.07	3.43	NA
	RS 504393	CCR2 chemokine receptor antagonist	6.71	2.35	yes
	JNJ 27141491	CCR2 chemokine receptor antagonist	NA	NA	yes
Neurotransmitters (dopamine/5-HT)	L-741,626	dopamine D2 receptor antagonist	10.76	2.21	no
	trifluprom azine	dopamine D2 receptor antagonist	9.25	2.07	no
	LP44	high-affinity 5-HT7 receptor agonist	6.45	2.20	no
	roxindole	agonist for D2,D3,D4 or HT1A	8.57	2.60	NA
	N-desmethylclozapine	5-HT2C antagonist	4.20	2.00	no
	R-96544	5HT2A antagonist	6.18	2.36	NA
Others	amiodarone	ion channel blocker; autophagy stimulator	4.85	3.40	yes
	loperamide	u-opioid receptor antagonist	5.17	2.05	yes
	KB-R7943 mesylate	NCX inhibitor; blocks TRPC channels	10.28	3.00	yes
	YM 244769	NCX inhibitor	NA	NA	yes

kinase C inhibitor, but recent reports show that GF109203X is also a potent inhibitor of DHCR24 (Luu et al., 2014). Our studies have found that U18666A, triparanol, and GF109203X increase levels of secreted and cell-associated apoE in primary human astrocytes (Table 1, Figures 2A, 2C, S2A, and S2B). Several other of our identified hits modulate 7-dehydrocholesterol reductase (DHCR7), which catalyzes the production of desmosterol and cholesterol from 7-dehydrodesmosterol and 7-dehydrocholesterol, respectively (Figure S3). AY-9944 and GANT61 have been described previously as enzymatic inhibitors as well as transcriptional inducers of 7-dehydrocholesterol reductase (DHCR7) (Lauth et al., 2010). Also, certain anti-depressant and anti-psychotic drugs, including the identified compounds haloperidol, clozapine, and chlorpromazine, have been described as modulators of DHCR7 protein via SREBP activation (Ferno et al., 2005; Raeder et al., 2006). Our studies have found that AY-9944, GANT61, haloperidol, chlorpromazine, and clozapine all increase levels of secreted as well as cell-associated apoE in primary human astrocytes (Table 1, Figures 2B, 2E, and S2C–S2F). Similar to previous reports (Ferno et al., 2005; Raeder et al., 2006; Lauth et al., 2010), our apoE-enhancing hit compounds also increase the protein levels of DHCR24 or DHCR7 (Figures 2C and 2E).

Previously reported apoE-inducing compounds belong largely to the family of nuclear receptor agonists, which co-induce ABCA1 and other ATP cassette transporters (Cramer et al., 2012; Liang et al., 2004; Zhao et al., 2014). Induction of ABCA1 appears to enhance lipidation and/or secretion of apoE and may contribute to β-amyloid-reducing pharmacological effects of LXR and RXR agonists. However, reports of the preclinical and clinical efficacy of previously identified nuclear receptor/ABCA1 agonists on AD pathology are mixed. To this end, we examined the effects of our hit compounds on ABCA1 induction, potentially discovering ABCA1-independent mechanisms. We found that both DHCR24- and DHCR7-modulating compounds increase apoE expression and secretion, with no induction of ABCA1 expression (Figures 2C–2F). We also identified additional apoE-promoting compounds in the absence of ABCA1 induction (Table 1), such as dopamine D2 receptor antagonists L-741,626 and trifluprom azine.

To explore whether increased apoE secretion by DHCR24/7 hit compounds act through the LXR pathway, human astrocytes were treated with LXR agonist compounds T0901317 or WAY252623, or DHCR24/DHCR7 regulators in the presence or absence of GSK 2033 (GSK) LXR inhibitor (Figures 2G and S5). As predicted, LXR agonist compounds T0901317 and WAY252623 increase apoE secretion, as detected by apoE ELISA. Upon addition of GSK 2033 LXR inhibitor, apoE secretion is suppressed (Figures 2G, S5A, and S5B). As demonstrated previously, treatment of human astrocytes with DHCR24 and DHCR7 hit compounds increase apoE secretion. However, upon addition of GSK 2033, apoE secretion levels are unaffected

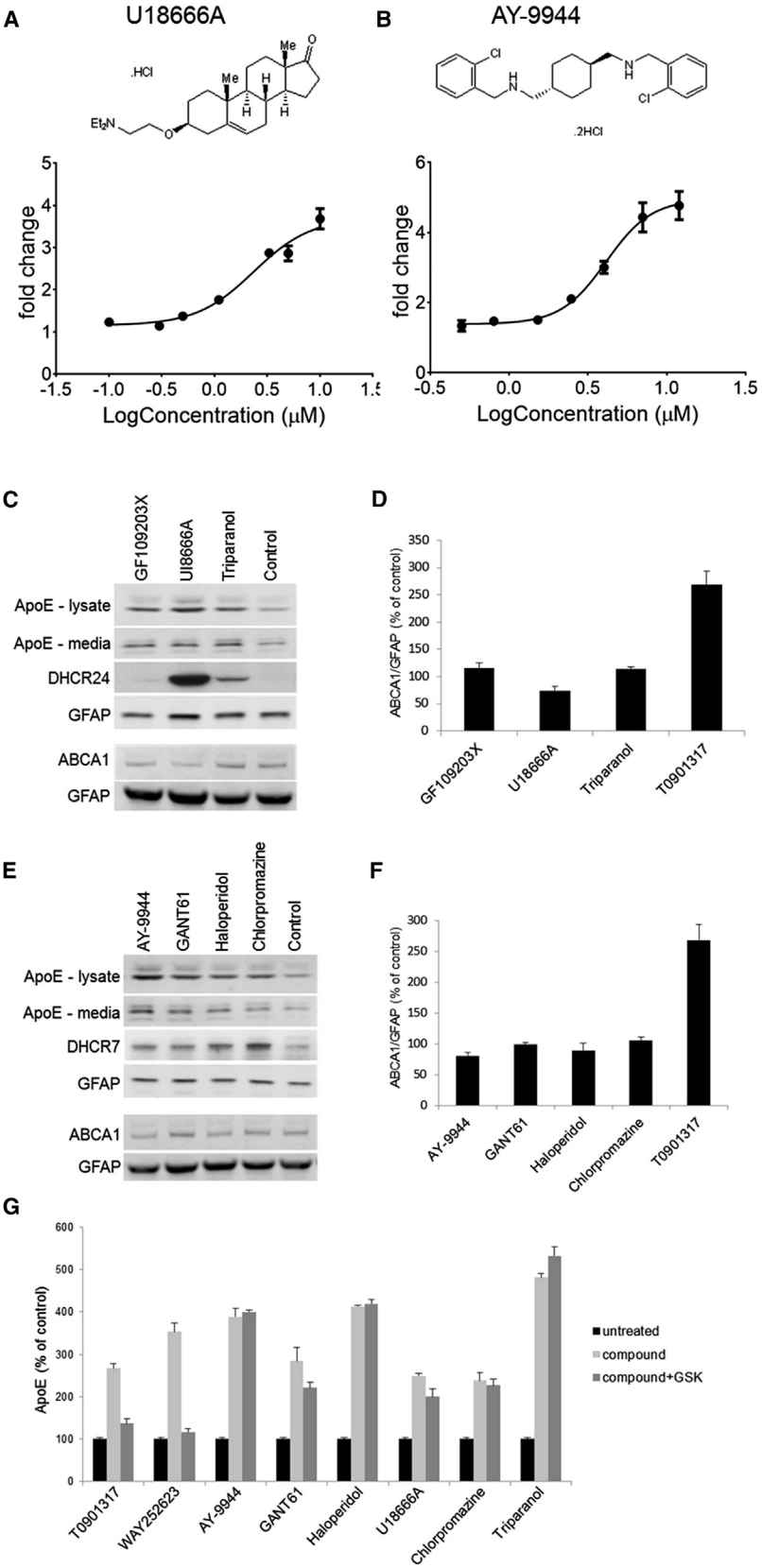

Figure 2. Effects of Small-Molecule Regulators of DCHR24 and DHCR7 on ApoE and ABCA1

(A) Chemical structure and dose-response curve of U18666A for secreted apoE on human astrocytes (EC_{50} = 2.35). n = 3 (mean ± SD).

(B) Chemical structure and dose-response curve of AY-9944 for secreted apoE on human astrocytes (EC_{50} = 4.12). n = 3 (mean ± SD).

(C) Representative western blot analyses of ABCA1, cell-associated apoE (lysate), secreted apoE (medium), DHCR24, and GFAP following treatment with the indicated DHCR24 inhibitors on human astrocytes.

(D) Quantification of ABCA1 induction following treatment with T0901317 and the indicated DHCR24 regulators on human astrocytes, n = 3 (mean ± SD). Anti-GFAP was used as loading control and normalization.

(E) Representative western blot analyses of ABCA1, cell-associated apoE (lysate), secreted apoE (medium), DHCR7, and GFAP following treatment with the indicated DHCR7 inhibitors on human astrocytes.

(F) Quantification of ABCA1 induction, following treatment with T0901317 and the indicated DHCR7 regulators on human astrocytes, n = 3 (mean ± SD). Anti-GFAP used as loading control and normalization.

(G) Effect of LXR inhibition on ABCA1 induction by DHCR24 and DHCR7 regulators. Human astrocytes were treated with compounds T0901317 or WAY252623 (LXR agonists) or DHCR24/DHCR7 regulators in the presence or absence of GSK 2033 (GSK), LXR inhibitor. Secreted apoE was analyzed by sandwich ELISA, n = 3 (mean ± SD).

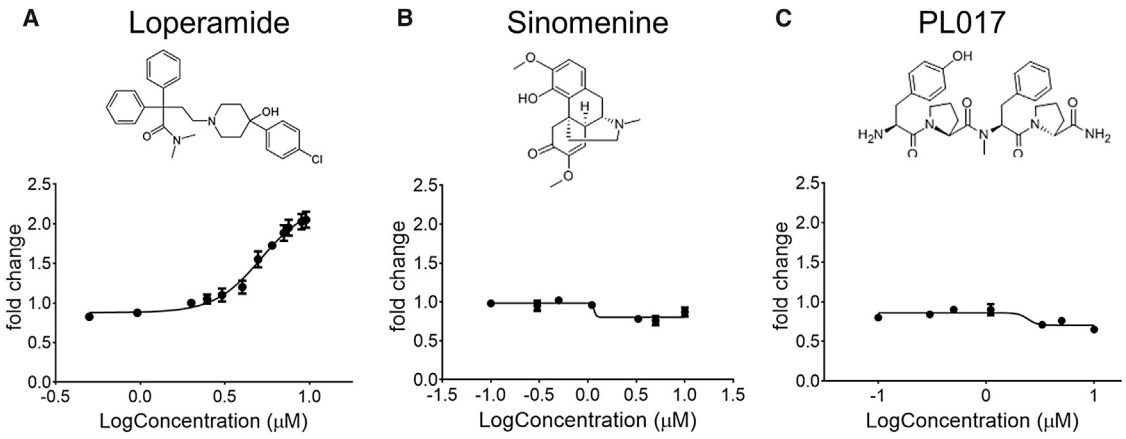

Figure 3. Pharmacological Effects of μ-Opioid Receptor Antagonists on ApoE Secretion in Primary Human Astrocytes

(A) Chemical structure and dose-response curve of loperamide, a μ-opioid receptor antagonist, for apoE (EC_{50}, 5.17 μM).

(B) Chemical structure and dose-response curve of simomenine, a μ-opioid receptor antagonist, for apoE.

(C) Chemical structure and dose-response curve of PL017, a μ-opioid receptor antagonist.

Data points represented as mean ± SD, n = 3.

(Figures 2G and S5C–S5H). These results further suggest that regulation of apoE secretion by DHCR24 and DHCR7 compounds does not act through the LXR-ABCA1-apoE regulatory axis.

Effects of DCHR24 and DHCR7 Modulators on Cholesterol Biosynthesis

It has been reported that certain cholesterol precursors and oxysterols might act as LXR ligands and contribute to the LXR-controlled signaling pathway, influencing apoE secretion (Abildayeva et al., 2006; Wang et al., 2008; Yang et al., 2006). We performed targeted sterol analyses to determine the correlative changes of cholesterol precursors (desmosterol and lathosterol), and the cholesterol metabolite 24S-hydroxycholesterol, in response to apoE-promoting DHCR24/7 regulators. We found that desmosterol levels were decreased by treatment with AY-9944, U18666A, triparanol, and T0901317, while lathosterol levels are increased by treatment with AY-9944, triparanol, GANT61, and T0901317 (Figure S4A). These data indicate that apoE-promoting chemical regulators of DHCR24/7 do indeed affect the levels of two major precursors of cholesterol biosynthesis. Cholesterol homeostasis and apoE modulation can further be regulated by oxysterols, such as 24S-hydroxycholesterol. There are many conflicting reports as to the role 24S-hydroxycholesterol plays in AD pathology, but 24S-hydroxycholesterol has been found to effect the expression, synthesis, and secretion of apoE (Leoni and Caccia, 2011; Lutjohann et al., 2000). Interestingly, 24S-hydroxycholesterol was decreased by all DHCR24/7 regulators, except for GF109303X (which had no effect) (Figure S4A).

To determine whether DHCR7/24 hit compound effects on cholesterol precursors, or 24S-hydroxycholesterol, could be responsible for increased apoE secretion, we treated human astrocytes with 24S-hydroxycholesterol, desmosterol, lathosterol, or T0901317. We also examined corresponding ABCA1 expression (Figure S4B). We found that all treatments increased ABCA1 expression, but only the LXR agonist, T0901317, increased apoE secretion and expression. These results suggest that DHCR7/24 hit compound effects on cholesterol precursors, or 24S-hydroxycholesterol, are not responsible for the previously observed increases in apoE secretion.

ApoE-Promoting Compounds with Previously Unknown Mechanisms

Our studies also identified a number of compounds that may induce apoE in human astrocytes via additional unknown mechanisms (Table 1). Loperamide, a well-known μ-opioid receptor antagonist, increased apoE secretion in astrocytes (Figure 3A). Given its structural resemblance to haloperidol (Figure S2D), it is conceivable that loperamide may confer apoE-stimulating effects by acting through a component in the sterol biosynthesis pathway, independently of the μ-opioid receptor. Indeed, we found that loperamide greatly increased lathosterol levels in astrocytes (Figure S4A). We also found that sinomenine and PL017, two structurally distinct μ-opioid receptor antagonists, had no effects on apoE levels, suggesting that the apoE-promoting action of loperamide is not dependent on the μ-opioid receptor (Figures 3B and 3C).

Antagonists of GPR14, also known as urotensin II receptor (UTS2R), were also identified as hit compounds, including SB657510 and GSK 1562590 (Figure 4). These compounds increased levels of both cell-associated and secreted apoE (Figures 4A–4C). GPR14 is expressed abundantly in the brain and has been implicated in atherosclerosis (Jegou et al., 2006; Tsoukas et al., 2011). Interestingly, urotensin II has recently been found to decrease ABCA1 expression in cultured macrophages (Wang et al., 2014). Our studies found that GPR14 antagonists induce ABCA1 expression (Table 1), suggesting a novel role for GPR14 in astrocytic apoE metabolism.

In Vivo Validation of Active Compounds Using Microdialysis

We next investigated if the DHCR24/7 modulators (U18666A or AY-9944) or loperamide confer apoE-enhancing effects in vivo.

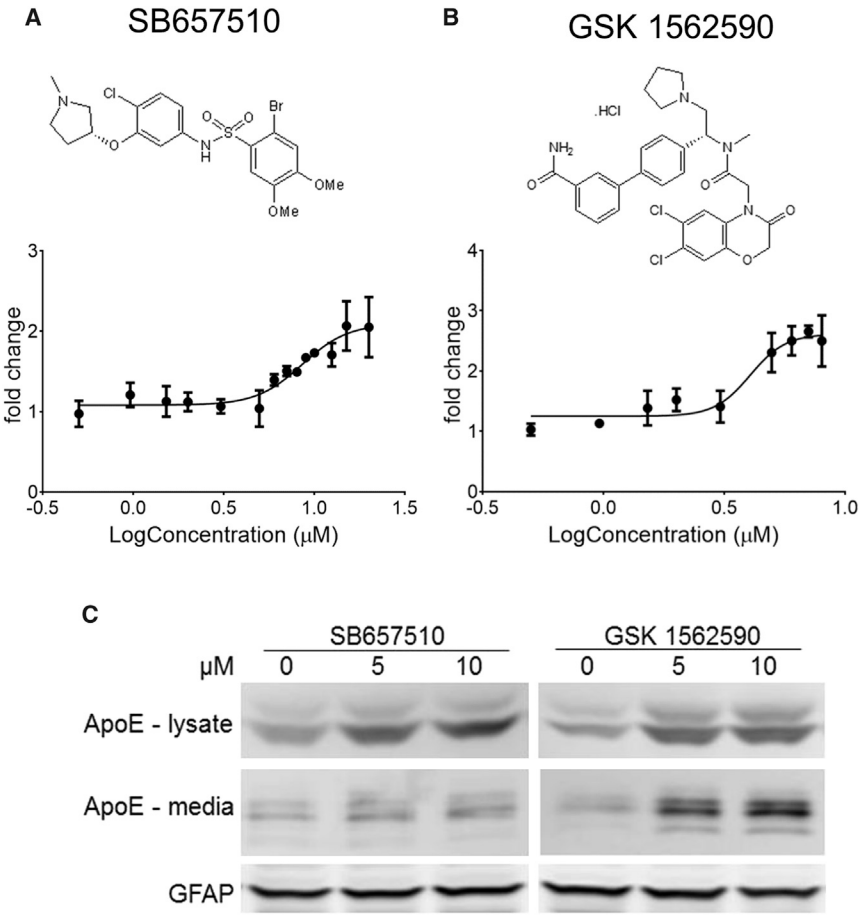

Figure 4. Induction of ApoE by Urotensin II Receptor Antagonists

(A and B) Chemical structure and dose-response curve of two antagonists of urotensin II receptor (UTS2R; also known as GPR14), SB657510 (A) and GSK1562590 (B). Data points represented as mean ± SD, n = 3.

(C) Western blot analysis of secreted or cell-associated apoE following treatment with SB657510 or GSK 1562590. Primary human astrocytes were incubated with the indicated compounds at 0, 5, or 10 μM and samples from the medium or lysates (cell-associated) were subjected to western blot analysis using anti-apoE and anti-GFAP as a loading control.

Since apoE secretion in vivo is difficult to assess using analysis of steady-state apoE levels in the brain, we employed in vivo microdialysis via a 1,000-kDa large-molecular-weight cutoff membrane to measure the apoE and Aβ levels in the brain ISF in the PS1/APP double transgenic mouse model of AD, awake and freely moving (Cramer et al., 2012; Ulrich et al., 2013). The compounds were administered directly into the brain by reverse dialysis through the probe. Administration of U18666A, AY-9944, and loperamide led to a time-dependent increase in apoE levels in the brain ISF (Figure 5A–5C). Inversely, correlative decreases in the levels of β-amyloid peptides harboring the C-terminal end at the position 40 ($A\beta_{x-40}$) were also observed in the samples treated with these compounds. Thus, our data support in vivo validation of hit compounds identified through HTS in human astrocytes.

Pharmacological Responses of ApoE-Promoting Compounds in Primary Astrocytes Verses an Astrocytoma Cell Line

We next investigated the differences in pharmacological responses between primary astrocytes and an astrocytoma cell line. We compared apoE-enhancing compounds in primary astrocytes from two separate human donors (both are *APOE3/3* genotype) versus human astrocytoma CCF-STTG1. Several compounds that were previously shown to increase apoE secretion, including retinoid 9-cis-RA, bexarotene, and T090317 (Liang et al., 2004; Zhao et al., 2014) exhibited positive activity in both primary human astrocytes and CCF-STTG1 cells, although the pharmacological responses were much greater in astrocytoma compared with primary astrocytes (Figure 6A). Among the identified hit compounds, we found that U188666A, GF109203X, AY-9944, GANT61, loperamide, and amiodarone stimulated apoE secretion in human astrocytes, but not in the astrocytoma cell line (Figure 6A), indicating that the cellular context of primary human astrocytes is critical for pharmacological activity in inducing apoE of these compounds. Viability assays were conducted in parallel to confirm that the observed apoE induction was not due to altered cell survival (Figure 6B).

DISCUSSION

The use of cellular models based on primary human cells offers significant value in establishing chemical biology and drug discovery assays with improved physiological relevance and translational potential (Finkbeiner et al., 2015). While primary cells serve as ideal systems for cell-based pharmacological screening, they are difficult to maintain and scale for HTS (An and Tolliday, 2010; Astashkina et al., 2012). Using cryopreserved primary human astrocytes, we have shown that these cells can be successfully adapted and scaled to 384-well-based HTS with robust Z factor values (Figure 1). Our current study describes, to our knowledge, the first example of HTS performed in primary human astrocytes; and we successfully identified new bioactive small-molecule regulators of apoE levels by conducting unbiased, phenotypic screening of drugs and bioactive compounds. A cell-based compound-screening effort for the identification of apoE stimulators has been described previously, using a transformed astrocytoma cell line CCF-STTG1 (Lee et al., 2011), but no screening results are publicly available and it is highly conceivable that a screen performed in astrocytoma can miss a number of hits that are preferentially active in primary cells. In addition, it is possible that a compound which is

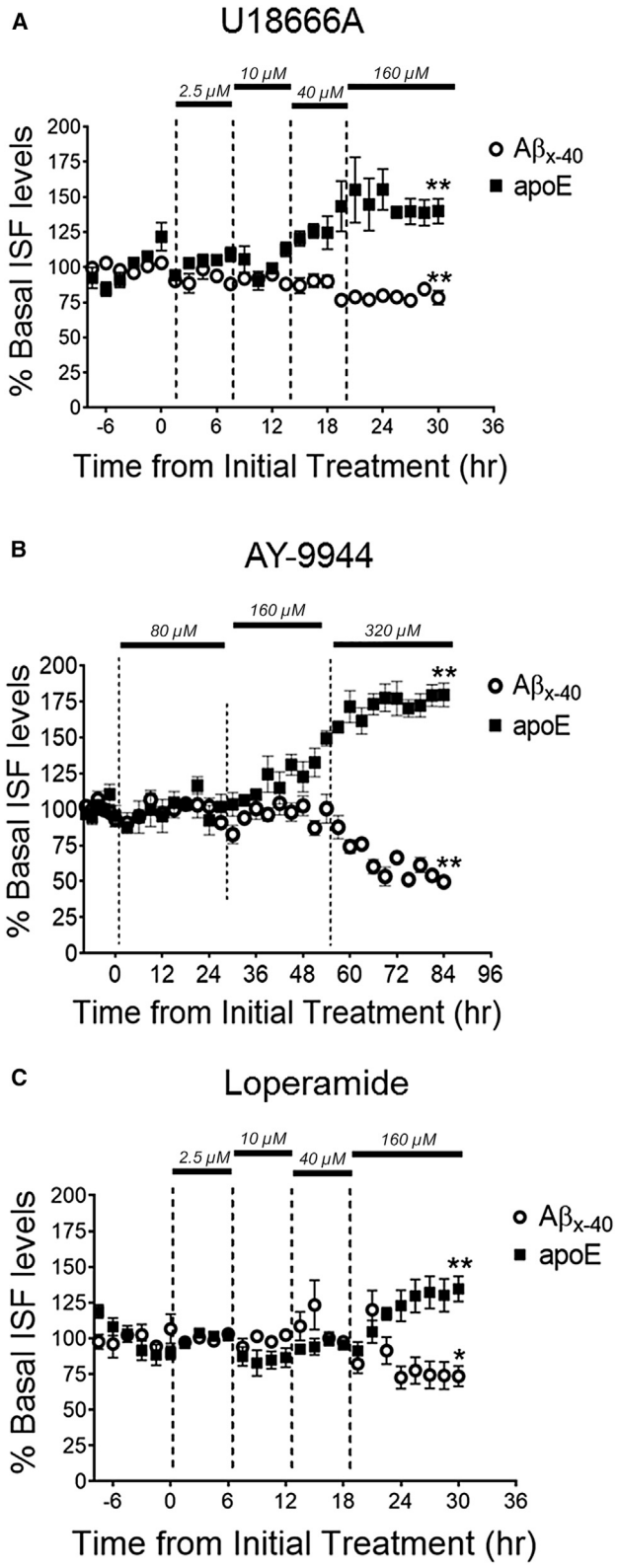

Figure 5. In Vivo Analysis of ApoE and Aβ Levels in Brain ISF by Microdialysis

(A) U18666A increases apoE (147.73% ± 9.61%) and decreases Aβ (78.24% ± 9.94%) levels in vivo using microdialysis, n = 4.

(B) AY-9944 increases apoE (179.56% ± 18.32%) and decreases Aβ (49.69% ± 3.92%) levels in vivo using microdialysis, n = 5.

(C) Loperamide increases apoE (141.82% ± 12.37%) and decreases Aβ (73.58% ± 14.13%) levels in vivo using microdialysis, n = 4. ISF $A\beta_{x-40}$ and apoE levels in the hippocampus of 2-month-old APP/PS1 mice were monitored using in vivo microdialysis with 1,000 kDa molecular weight cut off membranes. Following establishment of a 6-hr baseline, ISF level for $A\beta_{x-40}$ and apoE, mice were administered with U18666A (A) or loperamide (C) (injection concentrations into the probe are shown) and ISF $A\beta_{x-40}$ and apoE levels were assessed for an additional 30 hr. For AY-9944 (B), ISF $A\beta_{x-40}$ and apoE levels were assessed for an additional 78 hr.

*$p < 0.05$, **$p < 0.01$ compared with basal time 0 hr, Student's t test. Data points represented as mean ± SD.

cytotoxic to a transformed cell line, such as CCF-STTG1, might promote apoE secretion in primary astrocytes without affecting viability (or the inverse causality may be true), precluding identification in such a screen. Our current study indeed observed such phenomena, where certain compounds exert apoE-promoting activity only in physiological cells (i.e., primary human astrocytes), but not in transformed cell lines (i.e., CCF-STTG1). These findings demonstrate the importance of our approach in using physiologically relevant brain cells for phenotypic cell-based assays. Compared with an astrocytoma-based apoE assay, our use of primary human astrocytes exhibited comparable throughput assay adaptability in an HTS format despite the higher purchasing and maintenance costs associated with primary human astrocytes. Our HTS has yielded previously unknown pathways and targets that may carry important functional roles in regulating astrocytic apoE secretion.

One of the values of performing cell-based screening using annotated bioactive compound collections is being able to identify hits with known targets and establish a functional connection between the cell-based phenotype-of-interest (i.e., apoE secretion) and a novel regulatory pathway. We illustrate here that two key enzymes involved in cholesterol biosynthesis, DHCR24 and DHCR7, play a role in increased apoE secretion in vitro and in vivo, thereby functionally linking the cholesterol biosynthetic pathway to apoE regulation. DHCR24 and DHCR7 mediate multiple steps in cholesterol biosynthesis (Figure S3) and we have demonstrated that modulators of DHCR24 and DHCR7 regulate both cholesterol precursors and metabolites in our astrocytic cell system. Interestingly, these identified regulators of apoE expression and secretion do so in an ABCA1-independent manner, suggesting a new role for cholesterol biosynthesis in apoE production beyond the LXR-ABCA1-apoE regulatory axis (Koldamova et al., 2010).

In addition to small-molecule modulators of DHCR24 and DHCR7, our HTS revealed additional players in apoE production in human astrocytes. Other notable classes of compounds discovered in our HTS campaign include G-protein-coupled receptor modulators, such as the UTS2R (GPR14) antagonists, modulators of various neuroreceptors, as well as sodium/calcium channel regulators (Tables 1 and S2). The UTS2R antagonist is known to be expressed in astrocytes and has been linked to immune inflammation (Castel et al., 2006; Desrues et al., 2012; Liu et al., 2015). Given the anti-inflammatory functions associated with apoE, it is conceivable that apoE production and the urotensin system may crosstalk in response to inflammatory changes in the brain. In addition, our HTS campaign identified

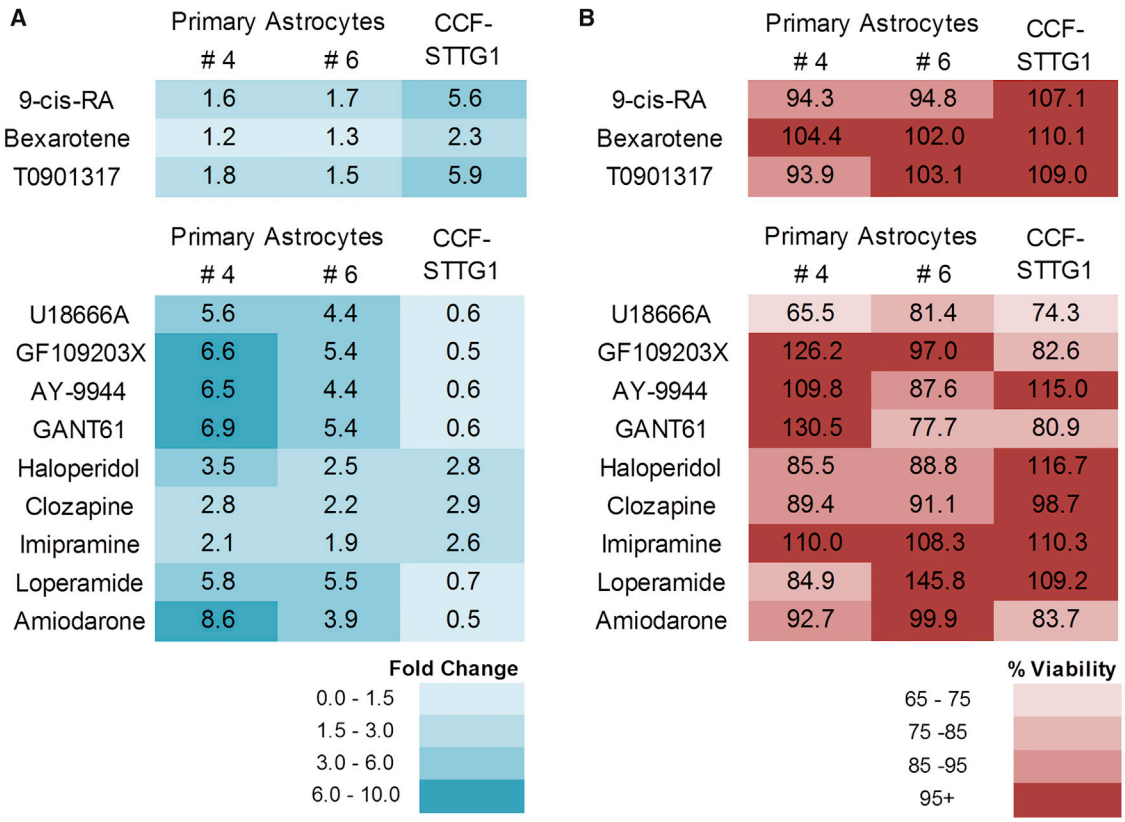

Figure 6. Comparison of Pharmacological Responses of Selected ApoE-Enhancing Compounds in Primary Human Astrocytes versus Astrocytoma

(A and B) Heatmaps of representative hits in primary human astrocytes from different donors (nos. 4 and 6) and CCF-STTG1, a commonly used astrocytoma cell line. Heatmaps show the highest observed fold increases (A) and corresponding viability (B).

various regulators of opioid, serotonin, dopamine, and histamine receptors. Most of these neuroreceptors have been associated with AD pathology and/or cognitive defects; although few have been implicated in apoE biology (Cirrito et al., 2011; Martorana and Koch, 2014; Thathiah and De Strooper, 2011; Zlomuzica et al., 2015). These identified compounds may serve as useful tools not only to investigate the regulatory mechanisms of astrocytic apoE, but also to help evaluate the significance of the pharmacological enhancement of apoE levels in AD-associated phenotypic changes in the brain, such as Aβ accumulation and neuroinflammation. Ultimately, identifying novel regulatory mechanisms of brain apoE metabolism may help to devise a new therapeutic strategy for AD.

SIGNIFICANCE

The use of physiologically relevant cellular models, such as human primary cells, offer significant value in establishing chemical biology and drug discovery assays with improved physiological relevance and translational potential. To our knowledge, no previous attempts have been made to discover the pharmacological agents that regulate apolipoprotein E (apoE) secretion in the context of physiological human brain cells, which may facilitate our efforts to explore complex underlying biological pathways. We took an unbiased high-throughput screening (HTS) approach to the discovery of new pharmacological agents that can induce apoE levels in human primary astrocytes. In the brain, apoE is synthesized and secreted mainly from astrocytes, and it has been postulated that the levels of brain apoE are critically associated with the pathophysiology of Alzheimer's disease. Our cell-based HTS of drugs and bioactive compounds identified small molecules that increase apoE in cultured human primary astrocytes via previously unknown mechanisms, including those not co-inducing ATP-binding cassette transporter 1. These include small-molecule modulators of key enzymes in the cholesterol biosynthetic pathway (e.g., DHCR7 and DHCR24). These newly identified compounds are active preferentially in human astrocytes but not in a popular astrocytoma cell line. Thus, our approach yielded previously unknown pathways that may carry important functional roles in regulating astrocytic apoE secretion and furnished new tools for investigating brain apoE biology.

EXPERIMENTAL PROCEDURES

Cell Culture

Primary human astrocytes, isolated from human cortex were purchased from (ScienCell). Each vial of cells, cryopreserved at passage one, can be used to

15 population doublings (roughly five passages). Two donors with APOE3/3 genotypes were used for comparison studies. Genotyping was performed by LGC. Astrocytoma cell line CFF-STTG1 was purchased from the ATCC. All cell lines were maintained as detailed by the manufacturer.

Compounds

The following libraries were used for the HTS campaign and are available in the Columbia HTS Core Facility (Scientific Director: Charles Karan): LOPAC, a collection of 1,280 pharmacologically active compounds (Sigma); spectrum collection, 2,000 biologically active and structurally diverse compounds from its libraries of known drugs, experimental bioactives, and pure natural products (MicroSource Discovery Systems); Tocriscreen, a collection of 1,279 biologically active compounds (Tocris); Prestwick Chemical Library, 1,200 small molecules, all of which are U.S. Food and Drug Administration (FDA)-approved drugs; John's Hopkins University Clinical Compound Library, 1,600 FDA- and foreign-approved drugs. The total number of screened compounds was 7,359 (75 compounds overlapped different libraries). All hit confirmation experiments were performed using newly purchased compounds from different vendors. These compounds were from Tocris, Cayman, Selleckchem, and Sigma.

Cell Viability Assay

Cell viability was measured in parallel using the CellTiter-Glo Cell Viability Assay Kit (BioAssay Systems).

ApoE ELISA

For HTS, we plated cells in 384-well plates and incubated them with compounds for 48 hr at a concentration of 10 μM, before performing sandwich ELISA (Mabtech). ELISA 384-well plates from (MaxiSorp 464718) were prepared by adding 50 μL of monoclonal antibody E276 diluted in PBS to 2 μg/mL for 24 hr at 4°C. The ELISA plates were then washed with PBS and blocked by adding 50 μL of blocking buffer (PBS with 0.05% Tween 20 containing 0.1% BSA). After incubating the plates for 24 hr at 4°C in the blocking buffer, all liquid was aspirated using BioTek ELx405 Select. Blocking buffer (10 μL) and 40 μL of the supernatant from the cell plates was then added to the ELISA plates and incubated for 24 hr at 4°C. The plates were then washed with blocking buffer and 50 μL of biotinylated monoclonal antibody E887 at 1 μg/mL was added to the plates and incubated for 1 hr at room temperature. The plates were then washed with blocking buffer and 50 μL of streptavidin-alkaline phosphatase diluted 1:1,000 in blocking buffer was added to the plates. The plates were then read by the EnVision 2104 for the baseline absorbance reading of the wells. After incubating at room temperature for 1 hr, the plates were washed and 50 μL p-nitrophenyl phosphate (pNPP) was added. The plates were shaken for 5 min at 600 rpm and allowed to sit at room temperature for 10 min. After a total of 15-min incubation time with the pNPP, the plates were read for absorbance at 405 nM.

Aβ ELISA

ISF $A\beta_{x\text{-}40}$ levels were measured using sandwich ELISAs as described previously (Cirrito et al., 2011). A mouse anti-$A\beta_{40}$ antibody (mHJ2) was used for capture, and a biotinylated central domain antibody (mHJ5.1), followed by streptavidin poly-HRP40 (Fitzgerald Industries), was used for detection. The ELISA was developed using Super Slow ELISA TMB (Sigma-Aldrich) and absorbance read on a Bio-Tek Epoch plate reader at 650 nm. The standard curve for the $A\beta_{x\text{-}40}$ ELISA was synthetic human $A\beta_{1\text{-}40}$ peptide (All American Peptide).

High-Throughput Screening

On day 1, 384-well tissue culture plates (Greiner 781080) were coated with 25 μL of poly-D-lysine (0.1 mg/mL) and incubated at 37°C for 1 hr. The plates were then washed with PBS and stored at 4°C. On day 2, the plates were seeded with 50 μL of cells at 200,000 cells/mL for a total of 10,000 cells per well. Cells were incubated with 5% CO_2 at 37°C for 24 hr. On day 3, following medium replacement, the Nanohead low-volume dispense head was then used to transfer 100 nL of compounds in DMSO at 5 or 10 mM stock concentration to the plates. The plates were incubated for 48 hr. Following incubation, 40 μL of the supernatant was aspirated from the plates using the PerkinElmer JANUS 384-well head equipped with p30 disposable tips. The supernatant was then added to apoE-coated ELISA plates. Recombinant apoE3 standard was also added to the ELISA plates to serve as a positive control. The viability of the cells after compound treatment was measured by adding 25 μL of CellTiter-Glo into the remaining volume of cell solution in the cell plates. The plates were then placed in the shaker for 5 min at 600 rpm and placed in the EnVision 2104 to read the luminescent counts per well. Initial screening was performed in triplicate at one concentration (10 μM) in triplicate. Initial "hit" compounds were defined as >2.0-fold change above the mean with a viability of >60%. "Hit" compounds were re-assayed at four different concentrations; and dose-response curves were generated to validate reproducibility and determine EC_{50} values using Prism software. Z′ factor was determined using the standard equation, defined as:

$$1 - \frac{3(\sigma_p + \sigma_n)}{|\mu_p - \mu_n|},$$

where σ_p and μ_p are the SD and the average of positive control-treated (T0901317 or amiodarone) samples, respectively; and σ_n and μ_n are the SD and the average of negative control-treated (DMSO) samples, respectively. Percentage of control (% of control) values were calculated by comparing the average measurement of compound-treated samples with that of DMSO-treated samples.

Analysis of Cholesterol Precursors

Cholesterol and non-cholesterol sterols were derivatized to trimethylsilyl ethers. Cholesterol was determined by gas-chromatography (GC)-flame-ionization detection and the non-cholesterol sterols and the oxysterol 24S-hydroxycholesterol by GC-mass-selective detection using 5a-cholestane- or epicoprostanolor deuterium-labeled 24S-OH-cholesterol, respectively, as internal standards (ISTD) as described previously (Lutjohann et al., 2000; Wang et al., 2008).

Western Blot Analysis and Antibodies

Proteins were resolved via SDS-PAGE using 4%–12% Tris/glycine gels, transferred to polyvinylidene fluoride, and probed for expression. Blots were detected using the Odyssey infrared imaging system (LI-COR Biosciences). Antibodies used include: anti-ApoE (Academy, catalog no. A01), anti-ABCA1 (GenScript, catalog no. A00121), anti-GFAP (Sigma, catalog no. SAB43000647), anti-DHCR7 (Santa Cruz, catalog no. sc-134500), and anti-DHCR24 (Santa Cruz, catalog no. sc-48477).

Immunocytochemistry

Astrocytes were fixed in 4% paraformaldehyde, permeabilized, and blocked for 1 hr in 10% normal goat serum or 10% fetal bovine serum. Primary antibodies were diluted in 10% normal goat serum containing 0.1% Triton X-100 and incubated overnight at 4°C. Detection antibodies include: anti-GFAP (Sigma), anti-GLAST-1 (Thermo Scientific, catalog no. PA5-19709) anti-CD44 (Sigma, catalog no. C7923), anti-TUJ1 (BioLegend, catalog no. 801201), and anti-MAP2 (Sigma, catalog no. M9942). Magnification: 20×. Following incubation of primary antibody, cells were washed and incubated for 1 hr at room temperature in Alexa Fluor 568- or 488-conjugated secondary antibody (Invitrogen). Immunostained cells were mounted, using VECTASHIELD Mounting Medium (Vector Laboratories), and imaged using the Nikon C1 Digital Confocal System.

Microdialysis

In vivo microdialysis was performed similar to Cramer et al. (2012). Mice were anesthetized using 1.5%–2.5% isoflurane, their heads shaved, and an anterior to posterior incision made along the midline of the head to expose the skull from several millimeters anterior of bregma to several millimeters posterior of lambda. The mouse was then mounted onto a manipulator arm-equipped small-animal stereotaxic apparatus (David Kopf Instruments). The skull was then leveled to within 0.1 mm at lambda, bregma, and two points 2.2 mm lateral of midline. A bore hole (0.75 mm diameter) was then created above the left hippocampus (bregma −3.1 mm, 2.5 mm lateral). A second bore hole (0.75 mm) was placed in the right, anterior quadrant of the skull in which to place an anchoring bone screw. An AtmosLM guide cannula (Eicom) was then stereotactically inserted into the left hippocampal formation (12° angle, dura mater −1.2 mm). The cannula was then secured into place using a binary

dental cement. The wound was then closed using surgical adhesive and the animal placed into a clean BASi Raturn Caging System (Bioanalytical Systems) designed to allow for free movement without placing stress on the Teflon tubing or probe apparatus and access to food and water ad libitum. Microdialysis probes (1,000 kDa; AtmosLM microdialysis probe, Eicom) were attached to a syringe pump on the inlet (KD Scientific) with a flow rate of 1.2 μL/min and a peristaltic pump on the outlet (MAB20, Scipro) with a flow rate of 1.0 μL/min. Probes were perfused with 0.15% BSA (Sigma-Aldrich) in artificial CSF, then inserted into the guide cannula so that the 2-mm tip of the probe was contained within the hippocampus. The mice were kept under constant light conditions throughout the experiment. Microdialysis samples were collected every 90 min throughout the study using a refrigerated fraction collector (Univentor 820 Microsampler, SciPro) then analyzed for $A\beta_{x-40}$ and apoE using sandwich ELISA immediately after each study. All experiment protocols using animals were performed in accordance with the guidelines established by the Animal Studies Committee at Washington University.

SUPPLEMENTAL INFORMATION

Supplemental Information includes five figures and two tables and can be found with this article online at http://dx.doi.org/10.1016/j.chembiol.2016.10.015.

AUTHOR CONTRIBUTIONS

G.M.F. and T.-W.K. conceived and designed the experiments and wrote the paper. G.M.F. performed the majority of the experiments. R.R. and C.K. performed automated HTS and provided intellectual input on HTS and hit analysis. D.L. performed lipid analysis and J.C. performed in vivo microdialysis. S.C. and N.W. provided critical intellectual input on overall design of experiments.

ACKNOWLEDGMENTS

We are grateful to J. Goldman and L.B.J. McIntire for helpful discussions. We are also grateful to H. Li for HTS optimization assistance and A. Kerksiek for GC-MS analysis of sterols. This work was supported by the U.S. NIH (NS074536 to T.-W.K.) and the Alzheimer's Drug Discovery Foundation.

Received: May 28, 2016
Revised: September 13, 2016
Accepted: October 25, 2016
Published: November 23, 2016

REFERENCES

Abildayeva, K., Jansen, P.J., Hirsch-Reinshagen, V., Bloks, V.W., Bakker, A.H., Ramaekers, F.C., de Vente, J., Groen, A.K., Wellington, C.L., Kuipers, F., et al. (2006). 24(S)-hydroxycholesterol participates in a liver X receptor-controlled pathway in astrocytes that regulates apolipoprotein E-mediated cholesterol efflux. J. Biol. Chem. *281*, 12799–12808.

An, W.F., and Tolliday, N. (2010). Cell-based assays for high-throughput screening. Mol. Biotechnol. *45*, 180–186.

Astashkina, A., Mann, B., and Grainger, D.W. (2012). A critical evaluation of in vitro cell culture models for high-throughput drug screening and toxicity. Pharmacol. Ther. *134*, 82–106.

Bellosta, S., Nathan, B.P., Orth, M., Dong, L.M., Mahley, R.W., and Pitas, R.E. (1995). Stable expression and secretion of apolipoproteins E3 and E4 in mouse neuroblastoma cells produces differential effects on neurite outgrowth. J. Biol. Chem. *270*, 27063–27071.

Castel, H., Diallo, M., Chatenet, D., Leprince, J., Desrues, L., Schouft, M.T., Fontaine, M., Dubessy, C., Lihrmann, I., Scalbert, E., et al. (2006). Biochemical and functional characterization of high-affinity urotensin II receptors in rat cortical astrocytes. J. Neurochem. *99*, 582–595.

Chen, H.K., Liu, Z., Meyer-Franke, A., Brodbeck, J., Miranda, R.D., McGuire, J.G., Pleiss, M.A., Ji, Z.S., Balestra, M.E., Walker, D.W., et al. (2012). Small molecule structure correctors abolish detrimental effects of apolipoprotein E4 in cultured neurons. J. Biol. Chem. *287*, 5253–5266.

Cirrito, J.R., Disabato, B.M., Restivo, J.L., Verges, D.K., Goebel, W.D., Sathyan, A., Hayreh, D., D'Angelo, G., Benzinger, T., Yoon, H., et al. (2011). Serotonin signaling is associated with lower amyloid-beta levels and plaques in transgenic mice and humans. Proc. Natl. Acad. Sci. USA *108*, 14968–14973.

Corder, E.H., Saunders, A.M., Strittmatter, W.J., Schmechel, D.E., Gaskell, P.C., Small, G.W., Roses, A.D., Haines, J.L., and Pericak-Vance, M.A. (1993). Gene dose of apolipoprotein E type 4 allele and the risk of Alzheimer's disease in late onset families. Science *261*, 921–923.

Cramer, P.E., Cirrito, J.R., Wesson, D.W., Lee, C.Y., Karlo, J.C., Zinn, A.E., Casali, B.T., Restivo, J.L., Goebel, W.D., James, M.J., et al. (2012). ApoE-directed therapeutics rapidly clear beta-amyloid and reverse deficits in AD mouse models. Science *335*, 1503–1506.

Dawson, M.I., and Xia, Z. (2012). The retinoid X receptors and their ligands. Biochim. Biophys. Acta *1821*, 21–56.

Desrues, L., Lefebvre, T., Lecointre, C., Schouft, M.T., Leprince, J., Compere, V., Morin, F., Proust, F., Gandolfo, P., Tonon, M.C., et al. (2012). Down-regulation of GABA(A) receptor via promiscuity with the vasoactive peptide urotensin II receptor. Potential involvement in astrocyte plasticity. PLoS One *7*, e36319.

Ferno, J., Raeder, M.B., Vik-Mo, A.O., Skrede, S., Glambek, M., Tronstad, K.J., Breilid, H., Lovlie, R., Berge, R.K., Stansberg, C., et al. (2005). Antipsychotic drugs activate SREBP-regulated expression of lipid biosynthetic genes in cultured human glioma cells: a novel mechanism of action? Pharmacogenomics J. *5*, 298–304.

Finkbeiner, S., Frumkin, M., and Kassner, P.D. (2015). Cell-based screening: extracting meaning from complex data. Neuron *86*, 160–174.

Fitz, N.F., Cronican, A., Pham, T., Fogg, A., Fauq, A.H., Chapman, R., Lefterov, I., and Koldamova, R. (2010). Liver X receptor agonist treatment ameliorates amyloid pathology and memory deficits caused by high-fat diet in APP23 mice. J. Neurosci. *30*, 6862–6872.

Fitz, N.F., Cronican, A.A., Lefterov, I., and Koldamova, R. (2013). Comment on "ApoE-directed therapeutics rapidly clear beta-amyloid and reverse deficits in AD mouse models". Science *340*, 924-c.

Fitz, N.F., Castranio, E.L., Carter, A.Y., Kodali, R., Lefterov, I., and Koldamova, R. (2014). Improvement of memory deficits and amyloid-beta clearance in aged APP23 mice treated with a combination of anti-amyloid-beta antibody and LXR agonist. J. Alzheimers Dis. *41*, 535–549.

Gabbi, C., Warner, M., and Gustafsson, J.A. (2014). Action mechanisms of liver X receptors. Biochem. Biophys. Res. Commun. *446*, 647–650.

Guo, L., LaDu, M.J., and Van Eldik, L.J. (2004). A dual role for apolipoprotein e in neuroinflammation: anti- and pro-inflammatory activity. J. Mol. Neurosci. *23*, 205–212.

Holtzman, D.M., Pitas, R.E., Kilbridge, J., Nathan, B., Mahley, R.W., Bu, G., and Schwartz, A.L. (1995). Low density lipoprotein receptor-related protein mediates apolipoprotein E-dependent neurite outgrowth in a central nervous system-derived neuronal cell line. Proc. Natl. Acad. Sci. USA *92*, 9480–9484.

Hong, C., and Tontonoz, P. (2014). Liver X receptors in lipid metabolism: opportunities for drug discovery. Nat. Rev. Drug Discov. *13*, 433–444.

Hu, J., LaDu, M.J., and Van Eldik, L.J. (1998). Apolipoprotein E attenuates beta-amyloid-induced astrocyte activation. J. Neurochem. *71*, 1626–1634.

Jegou, S., Cartier, D., Dubessy, C., Gonzalez, B.J., Chatenet, D., Tostivint, H., Scalbert, E., LePrince, J., Vaudry, H., and Lihrmann, I. (2006). Localization of the urotensin II receptor in the rat central nervous system. J. Comp. Neurol. *495*, 21–36.

Keene, C.D., Cudaback, E., Li, X., Montine, K.S., and Montine, T.J. (2011). Apolipoprotein E isoforms and regulation of the innate immune response in brain of patients with Alzheimer's disease. Curr. Opin. Neurobiol. *21*, 920–928.

Kim, J., Basak, J.M., and Holtzman, D.M. (2009). The role of apolipoprotein E in Alzheimer's disease. Neuron *63*, 287–303.

Kim, J., Yoon, H., and Basak, J. (2014). Apolipoprotein E in synaptic plasticity and Alzheimer's disease: potential cellular and molecular mechanisms. Mol. Cells *37*, 767–776.

Kockx, M., Jessup, W., and Kritharides, L. (2008). Regulation of endogenous apolipoprotein E secretion by macrophages. Arterioscler. Thromb. Vasc. Biol. *28*, 1060–1067.

Koldamova, R., Fitz, N.F., and Lefterov, I. (2010). The role of ATP-binding cassette transporter A1 in Alzheimer's disease and neurodegeneration. Biochim. Biophys. Acta *1801*, 824–830.

LaClair, K.D., Manaye, K.F., Lee, D.L., Allard, J.S., Savonenko, A.V., Troncoso, J.C., and Wong, P.C. (2013). Treatment with bexarotene, a compound that increases apolipoprotein-E, provides no cognitive benefit in mutant APP/PS1 mice. Mol. Neurodegener. *8*, 18.

LaDu, M.J., Shah, J.A., Reardon, C.A., Getz, G.S., Bu, G., Hu, J., Guo, L., and Van Eldik, L.J. (2001). Apolipoprotein E and apolipoprotein E receptors modulate A beta-induced glial neuroinflammatory responses. Neurochem. Int. *39*, 427–434.

Lauth, M., Rohnalter, V., Bergstrom, A., Kooshesh, M., Svenningsson, P., and Toftgard, R. (2010). Antipsychotic drugs regulate hedgehog signaling by modulation of 7-dehydrocholesterol reductase levels. Mol. Pharmacol. *78*, 486–496.

Leduc, V., Jasmin-Belanger, S., and Poirier, J. (2010). APOE and cholesterol homeostasis in Alzheimer's disease. Trends Mol. Med. *16*, 469–477.

Lee, J.A., Chu, S., Willard, F.S., Cox, K.L., Sells Galvin, R.J., Peery, R.B., Oliver, S.E., Oler, J., Meredith, T.D., Heidler, S.A., et al. (2011). Open innovation for phenotypic drug discovery: the PD2 assay panel. J. Biomol. Screen. *16*, 588–602.

Leoni, V., and Caccia, C. (2011). Oxysterols as biomarkers in neurodegenerative diseases. Chem. Phys. Lipids *164*, 515–524.

Liang, Y., Lin, S., Beyer, T.P., Zhang, Y., Wu, X., Bales, K.R., DeMattos, R.B., May, P.C., Li, S.D., Jiang, X.C., et al. (2004). A liver X receptor and retinoid X receptor heterodimer mediates apolipoprotein E expression, secretion and cholesterol homeostasis in astrocytes. J. Neurochem. *88*, 623–634.

Liu, C.C., Kanekiyo, T., Xu, H., and Bu, G. (2013). Apolipoprotein E and Alzheimer disease: risk, mechanisms and therapy. Nat. Rev. Neurol. *9*, 106–118.

Liu, L.M., Liang, D.Y., Ye, C.G., Tu, W.J., and Zhu, T. (2015). The UII/UT system mediates upregulation of proinflammatory cytokines through p38 MAPK and NF-kappaB pathways in LPS-stimulated Kupffer cells. PLoS One *10*, e0121383.

Lutjohann, D., Papassotiropoulos, A., Bjorkhem, I., Locatelli, S., Bagli, M., Oehring, R.D., Schlegel, U., Jessen, F., Rao, M.L., von Bergmann, K., et al. (2000). Plasma 24S-hydroxycholesterol (cerebrosterol) is increased in Alzheimer and vascular demented patients. J. Lipid Res. *41*, 195–198.

Luu, W., Zerenturk, E.J., Kristiana, I., Bucknall, M.P., Sharpe, L.J., and Brown, A.J. (2014). Signaling regulates activity of DHCR24, the final enzyme in cholesterol synthesis. J. Lipid Res. *55*, 410–420.

Lynch, J.R., Morgan, D., Mance, J., Matthew, W.D., and Laskowitz, D.T. (2001). Apolipoprotein E modulates glial activation and the endogenous central nervous system inflammatory response. J. Neuroimmunol. *114*, 107–113.

Mahley, R.W., and Huang, Y. (2012). Apolipoprotein e sets the stage: response to injury triggers neuropathology. Neuron *76*, 871–885.

Martorana, A., and Koch, G. (2014). Is dopamine involved in Alzheimer's disease? Front Aging Neurosci. *6*, 252.

Nathan, B.P., Bellosta, S., Sanan, D.A., Weisgraber, K.H., Mahley, R.W., and Pitas, R.E. (1994). Differential effects of apolipoproteins E3 and E4 on neuronal growth in vitro. Science *264*, 850–852.

Phillips, M.C. (2014). Apolipoprotein E isoforms and lipoprotein metabolism. IUBMB Life *66*, 616–623.

Pierrot, N., Lhommel, R., Quenon, L., Hanseeuw, B., Dricot, L., Sindic, C., Maloteaux, J.M., Octavea, J.N., and Ivanoiu, A. (2015). Targretin improves cognitive and biological markers in a patient with Alzheimer's disease. J. Alzheimers Dis. *49*, 271–276.

Pitas, R.E., Boyles, J.K., Lee, S.H., Hui, D., and Weisgraber, K.H. (1987). Lipoproteins and their receptors in the central nervous system. Characterization of the lipoproteins in cerebrospinal fluid and identification of apolipoprotein B,E(LDL) receptors in the brain. J. Biol. Chem. *262*, 14352–14360.

Raeder, M.B., Ferno, J., Vik-Mo, A.O., and Steen, V.M. (2006). SREBP activation by antipsychotic- and antidepressant-drugs in cultured human liver cells: relevance for metabolic side-effects? Mol. Cell Biochem. *289*, 167–173.

Ruiz, S., Brennand, K., Panopoulos, A.D., Herrerias, A., Gage, F.H., and Izpisua-Belmonte, J.C. (2010). High-efficient generation of induced pluripotent stem cells from human astrocytes. PLoS One *5*, e15526.

Saunders, A.M., Schmader, K., Breitner, J.C., Benson, M.D., Brown, W.T., Goldfarb, L., Goldgaber, D., Manwaring, M.G., Szymanski, M.H., McCown, N., et al. (1993). Apolipoprotein E epsilon 4 allele distributions in late-onset Alzheimer's disease and in other amyloid-forming diseases. Lancet *342*, 710–711.

Stansley, B., Post, J., and Hensley, K. (2012). A comparative review of cell culture systems for the study of microglial biology in Alzheimer's disease. J. Neuroinflammation *9*, 115.

Strittmatter, W.J., Saunders, A.M., Schmechel, D., Pericak-Vance, M., Enghild, J., Salvesen, G.S., and Roses, A.D. (1993). Apolipoprotein E: high-avidity binding to beta-amyloid and increased frequency of type 4 allele in late-onset familial Alzheimer disease. Proc. Natl. Acad. Sci. USA *90*, 1977–1981.

Tai, L.M., Koster, K.P., Luo, J., Lee, S.H., Wang, Y.T., Collins, N.C., Ben Aissa, M., Thatcher, G.R., and LaDu, M.J. (2014). Amyloid-beta pathology and APOE genotype modulate retinoid X receptor agonist activity in vivo. J. Biol. Chem. *289*, 30538–30555.

Tai, L.M., Ghura, S., Koster, K.P., Liakaite, V., Maienschein-Cline, M., Kanabar, P., Collins, N., Ben-Aissa, M., Lei, A.Z., Bahroos, N., et al. (2015). APOE-modulated Abeta-induced neuroinflammation in Alzheimer's disease: current landscape, novel data, and future perspective. J. Neurochem. *133*, 465–488.

Thathiah, A., and De Strooper, B. (2011). The role of G protein-coupled receptors in the pathology of Alzheimer's disease. Nat. Rev. Neurosci. *12*, 73–87.

Tsoukas, P., Kane, E., and Giaid, A. (2011). Potential clinical implications of the urotensin II receptor antagonists. Front Pharmacol. *2*, 38.

Ulrich, J.D., Burchett, J.M., Restivo, J.L., Schuler, D.R., Verghese, P.B., Mahan, T.E., Landreth, G.E., Castellano, J.M., Jiang, H., Cirrito, J.R., et al. (2013). In vivo measurement of apolipoprotein E from the brain interstitial fluid using microdialysis. Mol. Neurodegener. *8*, 13.

Vance, J.E., and Hayashi, H. (2010). Formation and function of apolipoprotein E-containing lipoproteins in the nervous system. Biochim. Biophys. Acta *1801*, 806–818.

Wahrle, S.E., Jiang, H., Parsadanian, M., Legleiter, J., Han, X., Fryer, J.D., Kowalewski, T., and Holtzman, D.M. (2004). ABCA1 is required for normal central nervous system ApoE levels and for lipidation of astrocyte-secreted apoE. J. Biol. Chem. *279*, 40987–40993.

Wang, N., Yvan-Charvet, L., Lutjohann, D., Mulder, M., Vanmierlo, T., Kim, T.W., and Tall, A.R. (2008). ATP-binding cassette transporters G1 and G4 mediate cholesterol and desmosterol efflux to HDL and regulate sterol accumulation in the brain. FASEB J. *22*, 1073–1082.

Wang, Y., Wu, J.F., Tang, Y.Y., Zhang, M., Li, Y., Chen, K., Zeng, M.Y., Yao, F., Xie, W., Zheng, X.L., et al. (2014). Urotensin II increases foam cell formation by repressing ABCA1 expression through the ERK/NF-kappaB pathway in THP-1 macrophages. Biochem. Biophys. Res. Commun. *452*, 998–1003.

Yang, C., McDonald, J.G., Patel, A., Zhang, Y., Umetani, M., Xu, F., Westover, E.J., Covey, D.F., Mangelsdorf, D.J., Cohen, J.C., et al. (2006). Sterol intermediates from cholesterol biosynthetic pathway as liver X receptor ligands. J. Biol. Chem. *281*, 27816–27826.

Yu, J.T., Tan, L., and Hardy, J. (2014). Apolipoprotein E in Alzheimer's disease: an update. Annu. Rev. Neurosci. *37*, 79–100.

Zerenturk, E.J., Sharpe, L.J., Ikonen, E., and Brown, A.J. (2013). Desmosterol and DHCR24: unexpected new directions for a terminal step in cholesterol synthesis. Prog. Lipid Res. *52*, 666–680.

Zhao, J., Fu, Y., Liu, C.C., Shinohara, M., Nielsen, H.M., Dong, Q., Kanekiyo, T., and Bu, G. (2014). Retinoic acid isomers facilitate apolipoprotein E production and lipidation in astrocytes through the retinoid X receptor/retinoic acid receptor pathway. J. Biol. Chem. *289*, 11282–11292.

Zlokovic, B.V. (2013). Cerebrovascular effects of apolipoprotein E: implications for Alzheimer disease. JAMA Neurol. *70*, 440–444.

Zlomuzica, A., Dere, D., Binder, S., De Souza Silva, M.A., Huston, J.P., and Dere, E. (2015). Neuronal histamine and cognitive symptoms in Alzheimer's disease. Neuropharmacology *106*, 135–145.